



# Fast-response optoelectronic detection of explosives' residues from the nitroaromatic compounds detonation: field studies approach

Jacek Wojtas<sup>a,\*</sup>, Robert Bogdanowicz<sup>b</sup>, Agata Kamienska Duda<sup>c</sup>, Beata Pietrzyk<sup>a</sup>, Michał Sobaszek<sup>b</sup>, Piotr Prasuła<sup>c</sup>, Anna Dettlaff<sup>b</sup>, Krzysztof Achtenberg<sup>a</sup>

<sup>a</sup> Institute of Optoelectronics, Military University of Technology, 00-908 Warsaw, Poland

<sup>b</sup> Faculty of Electronics, Telecommunications and Informatics, Gdansk University of Technology, 80-233 Gdansk, Poland

<sup>c</sup> Military Institute of Armament Technology, 05-220 Zielonka, Poland

## ARTICLE INFO

### Article history:

Received 23 January 2020

Received in revised form 8 April 2020

Accepted 1 May 2020

Available online 13 May 2020

### Keywords:

Trace explosives detection  
Nitrogen-based explosives' detection  
Nitroaromatic compounds detection  
Explosives' detonation  
Post-explosion residues detection  
HEM detection  
Laser absorption spectroscopy  
CEAS  
NO<sub>2</sub> detection  
NO<sub>2</sub> analyzer

## ABSTRACT

We are presenting an application of optoelectronic nitrogen dioxide (NO<sub>2</sub>) analyzer based on cavity enhanced absorption spectroscopy in the detection of traces of explosives after detonation. It has been shown that the analyzer using blue-violet laser is able to detect explosive residues after the detonation of various amounts of nitroaromatic compounds (75 g–1 kg) with higher efficiency than the HPLC soil sample testing equipment, which is the common standard in the analysis of explosives. Field studies have shown that it provided quick results, the amplitudes of which were about 8 dB despite the fact that NO<sub>2</sub> in the air was 3 orders of magnitude smaller than explosives found in soil. The NO<sub>2</sub> concentration after an explosion of different explosives at the distance of up to 20 m from the crater was 21–137 ppb, which was also dependent on the time between the explosion and the measurement, temperature and humidity of the atmospheric air and wind speed.

© 2020 The Author(s). Published by Elsevier Ltd. This is an open access article under the CC BY-NC-ND license (<http://creativecommons.org/licenses/by-nc-nd/4.0/>).

## 1. Introduction

The post-explosion residues detection techniques are extremely useful in investigations of the causes of an explosion, i.e. the detection of the source of energy release in result of detonation of an explosive, deflagration or physical burst [1]. The nitrogen dioxide optoelectronic analyzers could be applied for the detection of high explosives materials (HEM) characterized by low vapor pressure [2,3], which commonly used in various explosive devices (ED) or improvised devices (IED). These types of analyzers are supporting high-performance liquid chromatography (HPLC) that is extensively used for the analysis of explosives. HPLC is standardized by the U.S. Environmental Protection Agency (EPA) [4,5] for monitoring nitroaromatic explosives in soils, grounds water and sediments, for detecting ppb levels of some explosive residues. HPLC enables the selective determination of various types of explosive compounds, not only those containing nitro groups, but due to the use of various types of chromatographic columns and

appropriate detectors, basically all types of commonly used explosives [6]. Fast preliminary detection (with the optoelectronic analyzer) of nitrogen compounds and double identification of samples with use of the HPLC method give a broader information about the tested explosive-contaminated samples. Obviously, it is critically important to answer promptly what kind explosive material was used at the crime scene or other terroristic act. Rapid detection of specific explosives or other hazardous materials makes possible to start the immediate response of services or perform the evacuation of threatened civil persons. The application of optoelectronic NO<sub>2</sub> analyzer providing high sensitivity, high selectivity and fast response. The indirect detection of explosion residues by studying nitrogen dioxide traces has been previously reported. Ulf Nyberg et al. [7] described the experiments related to detonation of pure emulsion explosives E682 (with additives of 5% Al and with 30% dry ANprills) in a 35 m<sup>3</sup> blasting chamber. They measured the concentration of CO and NO<sub>x</sub> emissions for approximately ½ hour with a flue gas analyzer. Results for NO concentrations were obtained in the range of few to several dozen ppm and 0 ppm for NO<sub>2</sub> for most measurements. Explosive fumes have also been studied by Mainiero et al. [8] who examined the risk of toxic emissions from

\* Corresponding author.

E-mail address: [jacek.wojtas@wat.edu.pl](mailto:jacek.wojtas@wat.edu.pl) (J. Wojtas).

blasting. He discovered, among the other things, that the amount of toxic fumes depends strongly on the explosive's composition, confiner, age and contamination agents such as water, drill cuttings etc.

Sapko et al. [9] have studied the chemical and physical factors influencing on nitrogen oxides ( $\text{NO}_x$ ) associated with non-ideal detonation. They observed the NO concentration of 50–150 ppm during the detonation of explosives in a 274 m<sup>3</sup> vacuum chamber. Samples were taken from the vapors for 73 minutes. During this time, the NO concentration dropped from 185 ppm to 26 ppm due to the formation of  $\text{NO}_2$  in contact with  $\text{O}_2$ . The  $\text{NO}_2$  concentration was more stable and dropped from 70 ppm to 43 ppm. NO and  $\text{NO}_2$  were measured using a chemiluminescent analyzer.

The research related to the determination of  $\text{NO}_x$  was also presented in [10]. Explosives were detonated in a blast chamber consisting of classic steel mortar. The concentration of NO and  $\text{NO}_2$  in the samples was recorded for 20 minutes using a chemiluminescent analyzer (TOPAZE 32M Environnement). Depending on the type of explosive, the NO concentration was between 0.4 and 5.5 l/kg and the one of  $\text{NO}_2$  between 0.02 and 4.5 l/kg.

In the research report of the Health and Safety Executive (HSE) [11], two MultiRAE chemical detectors were selected due to their robust construction and the possibility of resolution below ppm. They carried out measurements of  $\text{NO}_2$  concentration at the distance of 100 m for different mass of explosives and at different times from the explosion. For example, the  $\text{NO}_2$  concentration was between 32 ppm for 83 kg of explosives (and after about 8.17 minutes) and 275 ppm for 102 kg of explosives (and after about 6.42 minutes). The described experiments were carried out in special chambers or with use of high-mass samples.

There are also publications describing the use of laser absorption spectroscopy to study residue after the explosion of explosives weighing 14 g [12,13]. The object of the study were gas detonation products of solid charges PETN, PBXN-5 and CompB, which were pressed into cylindrical pellets and NM-AP that was a slurry of liquid nitromethane and ammonium perchlorate powder. Gases such as CO,  $\text{CO}_2$ ,  $\text{H}_2\text{O}$  and  $\text{N}_2\text{O}$  were studied by direct absorption spectroscopy setup equipped with a mid-infrared external cavity quantum cascade laser, the lasing wavelength of which was swept repeatedly over a range of 4.35–4.88  $\mu\text{m}$ . The tests were carried out in a 2.5 m<sup>3</sup> chamber providing the optical path length of 1.17 m. The authors presented spectral characteristics of absorbance and gas column density values. The highest density was recorded for  $\text{CO}_2$  (maximum value:  $29 \times 10^{18} \text{ cm}^{-2}$ ) and the lowest for  $\text{N}_2\text{O}$  (maximum value:  $44 \times 10^{15} \text{ cm}^{-2}$ ).

Our goal was to show the ultra-sensitive laser analyzer enabling detection of HEM traces in field tests as a new useful tool for exploring explosive sites. Thanks to the advantages of laser absorption spectroscopy, the investigation can be carried out in a very short time at the scene of the incident, and without the need for special sampling and delivery to the analytical laboratory. It should also be emphasized that, to the best of our knowledge, this is the first demonstration of an optoelectronic analyzer using a blue-violet laser to detect explosive residue after the detonation of small amounts of nitroaromatic compounds in the open space.

## 2. Materials and methods

As a part of the military field tests, studies were carried out with use of commercially available secondary high explosives (Fig. 1a) such as: TNT and RDX, which can also be obtained from unexploded ordnance and then reused. TNT is relatively safe to handle and is classified as low melting explosive easy to melt from ammunition. RDX is more powerful explosive than TNT, due to higher velocity of detonation and detonation pressure. The charges were

made to map the use of explosives in real conditions. Training ground of Military Institute of Armament Technology (Fig. 1b) as well as scenarios and samples of different explosives were prepared by NATO experts from Military Institute of Armament Technology (Zielonka, Poland). The following explosives samples were used during the tests:

- pressed TNT, 75 g boosters (1.59 g/cm<sup>3</sup>),
- cast TNT, 1 kg charge (1.50 g/cm<sup>3</sup>),
- cast RDX/TNT 50/50 weight ratio, 1 kg charge (1.69 g/cm<sup>3</sup>),
- pressed A-IX-1, RDX phlegmatized with WAX, 1 kg charge (1.62 g/cm<sup>3</sup>).

The prepared explosives samples were remotely initiated with use of standard ERG electric detonators and electronic capacitor exploder EZK-100 (BELMA S.A, Poland). In all attempts, the explosive was fully detonated and an explosion crater of various sizes was created, depending on the mass and type of explosive used. After each test, air (optoelectronic  $\text{NO}_2$  analyzer, Fig. 2a) and soil samples (for HPLC) containing the residues after the explosion were taken, at different distances from the explosion site, and from the explosive crater, to obtain a representative number of samples broken down by place of collection. This treatment was aimed at assessing the diversity of the HE trace content in the explosion crater. As a part of the experiment, a set of 4 witness plates (metal covers) distant from the place of placing the charge by 1 m was also used (Fig. 2b), whose task was to “catch” the HE residue, which during the detonation could be thrown off the place of charge initiation.

### 2.1. Portable optoelectronic $\text{NO}_2$ analyzer design

Many papers are dedicated to optoelectronic detection of nitrogen dioxide in mid-infrared (MIR) range of wavelength [14–16]. As it was shown in Fig. 3, the absorption spectrum of this compound has also a band in visible range of light, where the electronic transitions are observed. The maximum of the absorption cross section varies from values of about  $3.5 \times 10^{-19}$  to  $8 \times 10^{-19} \text{ cm}^2$  (at 293K). In this wavelength ranges, no absorption interferences from other gases or vapors existing in the standard atmospheric air have been noticed [17].

In contrast to MIR, such solution enables to avoid the interferences induced by other gases existing in the atmosphere, especially  $\text{H}_2\text{O}$  or  $\text{CO}_2$ . Moreover, precise matching of the laser spectrum to selected absorption line is crucial for the sensitivity and selectivity of MIR gas sensors. For this purpose, expensive systems using quantum cascade lasers (QCL) that have to be precisely tuned to the desired wavelength by accurate setting of temperature and driving current have been applied. Laboratory constructions of high-sensitivity optoelectronic sensors of  $\text{NO}_2$  have been already demonstrated [18].

Here we are presenting our compact optoelectronic analyzer (dimensions: 95 × 69 × 37 cm, weigh: 35 kg) that was developed with use of blue-violet laser diode for  $\text{NO}_2$  detection. Its design is similar to its previous setup [3,19], but now it is equipped with additional possibilities of field research aimed at detecting traces of explosive residues after the detonation of nitroaromatic compounds. The operation idea of the analyzer based on cavity enhanced absorption spectroscopy (CEAS) that was proposed in 1998 by Engeln et al. [20], which belong to the one of the most sensitive laser absorption spectroscopy method. It combines the advantages of selective and fast measurements using a laser, extreme sensitivity and stability resulting from the excitation of dense structure of weak modes in a high-quality optical cavity, and differential concentration measurement based on the decay times of radiation in the cavity. Simplified scheme of the



Fig. 1. Photo of explosives samples for tests (a) and MIAT explosive test area: marked distance (60 m) of the bunker from the explosive site (b).

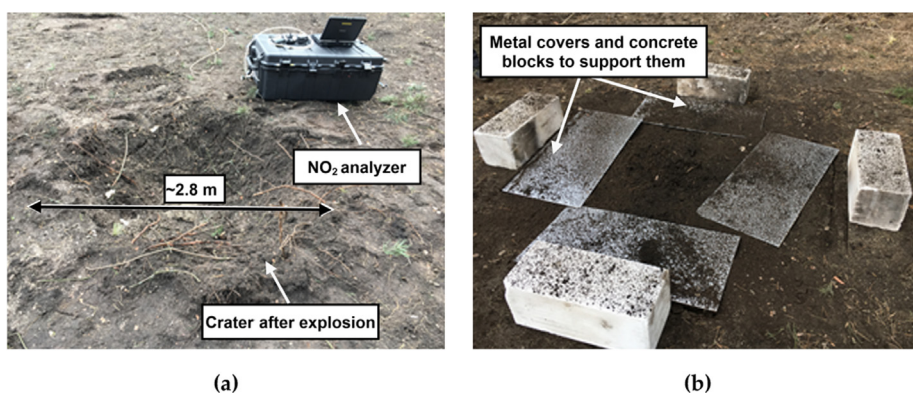


Fig. 2. Photos of optoelectronic NO<sub>2</sub> analyzer near the crater after the explosion (a), metal plates after the explosion between them (b).

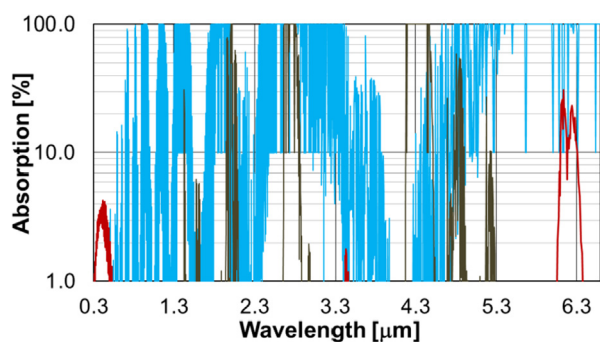


Fig. 3. High-resolution transmission molecular absorption database (HITRAN) simulation of absorption spectra: 21.6 ppb NO<sub>2</sub> – red line,  $6.257 \times 10^3$  ppm H<sub>2</sub>O (49.1%RH, 10.6 °C) – blue line and  $3.3 \times 10^2$  ppm CO<sub>2</sub> – black line, simulation performed at 1 atm and 10.6 °C for 1000 m pathlength. (For interpretation of the references to colour in this figure legend, the reader is referred to the web version of this article.)

optoelectronic NO<sub>2</sub> analyzer has been shown in Fig. 4. Its main elements are: pulsed blue-violet diode laser (TopGaN, Poland) operating at 414 nm, a sample chamber (optical cavity) that was fixed to the optical plate and sensitive photoreceiver. The wavelength used minimizes the photolysis effect [21] compared to systems with a 405 nm laser [22,23]. Parameters of laser pulses were: 50 ns FWHM duration time, 500 mW peak power, 1 kHz repetition rate. The cavity was constituted by two mirrors (CRD Optics Inc.) the reflectivity of which is better than 0,9999 at the wavelengths of

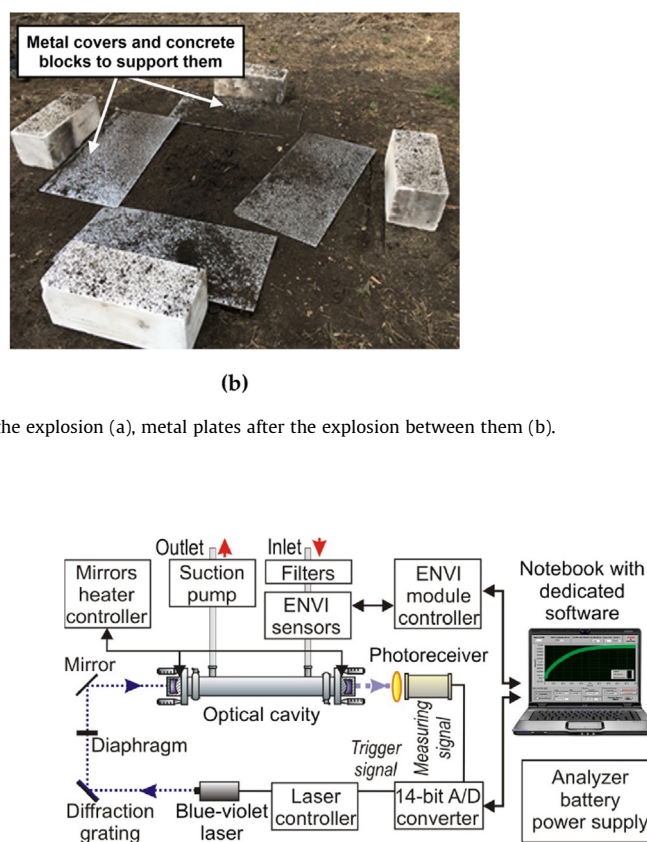


Fig. 4. Scheme of portable optoelectronic NO<sub>2</sub> analyzer.

$410 \pm 15$  nm. Their radius of curvature is 1 m while the distance between them is of 50 cm. The mirrors are mounted in two hermetic gimbals which are fixed to frontal surfaces of the chamber. All metal elements of the chamber were made of stainless steel, providing the reducing of gas adsorption on the walls. The air samples were transported using PTFE pipes. Adjacent surfaces of the parts were sealed up with O-rings. The output signal (leakage radiation from the cavity) is registered by a photomultiplier R7518 (Hamamatsu, Japan). The acquisition of the experimental signal is achieved with two channel 14-bit A/D converter (Cleverscope, New Zealand). The analysis of signals and determination of NO<sub>2</sub> concentration by temporal Q-factor determination is performed with dedicated LabVIEW software [19].

The investigated air enters to the chamber perpendicularly to the light beam through the inlet located in the top cover and leaves the chamber through the outlet located on the opposite side of its housing. The total volume of the chamber and tubes is about 0.5 l. The light scattering by some aerosols and smokes existing in the air is reduced due to application of a particulate and coalescence filters. Moreover the mirrors of the cavity are heated to the temperature of 50 °C in order to avoid water vapor condensation on their surface. To control inlet gas samples parameters, the optoelectronic NO<sub>2</sub> analyzer has been equipped with dedicated ENVI module (Fig. 5a) including sensor HYT271 (Innovative Sensor Technology IST AG, Switzerland) measuring temperature and relative humidity, barometric sensor MS5607 (Measurement Specialties, Inc., USA) measuring pressure, and with FS5 Thermal Mass flow sensor (IST AG, Switzerland). The validation and calibration of sensors were carried out with use of Brooks Instruments Read Out & Control Electronics 0152 controller equipped with Brooks DELTA Smart II Mass Flow and DELTA Smart II Pressure. As to the relative humidity (RH) sensor, 491M-HG (KIN-TEK Laboratories Inc., USA) was applied to produce reference gas sample with a moisture content of about 10% to 90% with an accuracy of ±3% (Fig. 5b). All sensors of ENVI module were integrated and synchronized with the optoelectronic NO<sub>2</sub> analyzer system with use of 8-bit microcontroller. The module has been also equipped with the SD card data storage, external temperature sensors inputs, USB and RS-485 interfaces. It has a compact construction and low energy consumption.

In Fig. 6 we demonstrate the results of the optoelectronic NO<sub>2</sub> analyzer tests with reference to NO<sub>2</sub> samples in various concentrations. The samples of controlled N<sub>2</sub> - NO<sub>2</sub> mixtures (5-350 ppb) were prepared with use of the 491M type gas standards generator (KIN-TEK Laboratories Inc., USA) providing high accuracy of calibration samples, which did not exceed 6.9% in the selected concentration range [24].

In order to ensure a good signal to noise ratio the registration was averaged over 1280 of laser pulses (resulting in the

optoelectronic NO<sub>2</sub> analyzer response time of 1.8 s). When no absorber was in the cavity, we observed the decay time  $\tau_0 = (13.6 \pm 0.2) \mu\text{s}$  that is equivalent to optical cavity length of  $(4077 \pm 60) \text{ m}$ . Then the cavity was connected with the gas standards generator. Good consistence was achieved between the measured absorption coefficients and the one calculated for corresponding NO<sub>2</sub> concentrations when the absorption cross section of  $5.5 \cdot 10^{-19} \text{ cm}^{-2}$  has been assumed. As shown, the coefficient of determination ( $R^2$ ) reached values exceeding 0.999, which indicates high adequacy of linear regression (Fig. 6a). Above 10 ppb, the differences between the concentrations measured with the analyzer and reference samples are below 10% (Fig. 6b).

## 2.2. HPLC measurement procedure

The reverse-phase high-performance liquid chromatography (RP-HPLC) was used to analyze the explosives residues in the collected material (soil) as a reference to the optoelectronic NO<sub>2</sub> analyzer tests. The analysis of the samples was carried out with use of the Prominence-i LC 2030 3 D (Shimadzu, JP) system equipped with Kinetex 00B-4601-E0 type column (Phenomenex Inc.), UV photodiode array spectrophotometric detector (PDA) in accordance with the recommendations of ASTM procedures for the analysis of nitroaromatic and nitramin explosives in soil [25]. The gradient RP-HPLC system configuration was applied. The mobile phases A and B consisted of 0.1% trifluoroacetic acid (TFA) in water and 0.1% TFA in acetonitrile. The total run time was 50 min at a flow rate of 1.0 mL/min and at a temperature of 25 °C. PDA allows the dual identification of the sample by determining the retention time of the sample tested and the collection of the UV spectrum and its comparison with the standard data. Instrument control and data acquisition were performed with use of the Lab Solution software (Shimadzu, Japan).

The analysis of the samples taken from the ground required also information on the limits of quantitation (LOQ) specified for the signal-to-noise ratio (SNR) of 10 and limits of detection (LOD)

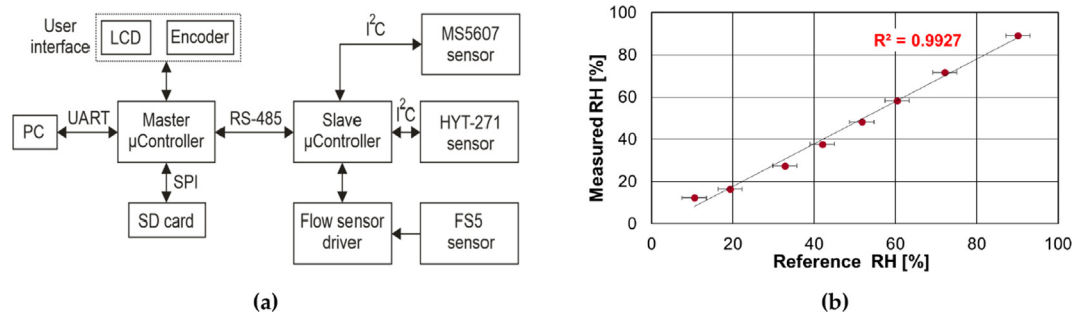


Fig. 5. Scheme of the ENVI module (a) and sample results of calibration of the RH sensor (b).

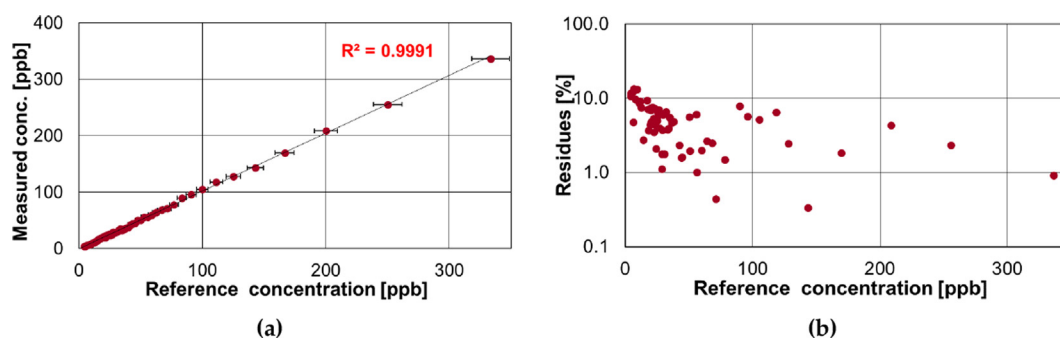


Fig. 6. Measured concentration of nitrogen dioxide with developed optoelectronic NO<sub>2</sub> analyzer versus the mixing ratio of N<sub>2</sub>-NO<sub>2</sub> mixtures.

specified for SNR = 3. The standard solutions were diluted to get a series of concentrations from 0,3 μg/mL to 70 μg/mL to determine these parameters. The standards RDX and TNT, which were used in research were taken from Accu Standard, InC, USA company (Figs. 7 and 8).

### 3. Results

#### 3.1. Field tests of the optoelectronic NO<sub>2</sub> analyzer

After the explosion of each of four samples, carried out in accordance with the assumed scenarios and safety procedures, the NO<sub>2</sub> analyzer was moved by two persons to the test site, where the air samples were taken directly for NO<sub>2</sub> concentration measurements.

The measurements were carried out for each sample at 3 or 4 different distances from the explosion crater: 20 m, 10 m, 1 m, 0 m, and for a sample taken from a PTFE film attached to one of 4 metal covers (Fig. 9). The analyzer operated in a continuous measurement mode and determined every 1.8 s as to the NO<sub>2</sub> concentration in the currently collected air sample. The air was taken via a built-in pump at a speed of 1 l/min. Due to the volume of 0.5 l of the entire pneumatic system of the analyzer, it was necessary to get 30 seconds to fill the volume of the pneumatic part of the analyzer and reach the NO<sub>2</sub> concentration at the test site. Therefore, all measurements were recorded for 1 minute. The start of each measurement depended on the safety procedures, time required to stabilization of measurement conditions at the explosion site and to relocate and prepare the analyzer and equipment. In addition, after each test, the analyzer was verified using calibration gas.

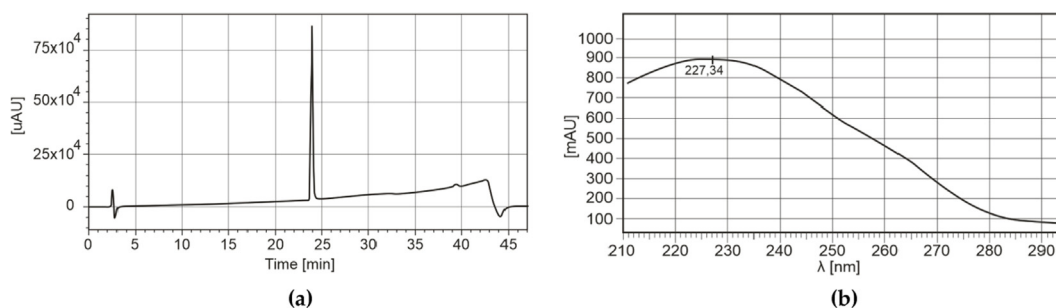


Fig. 7. TNT standard chromatogram (a), UV spectrum of TNT standard at retention time of 23.9 min (b).

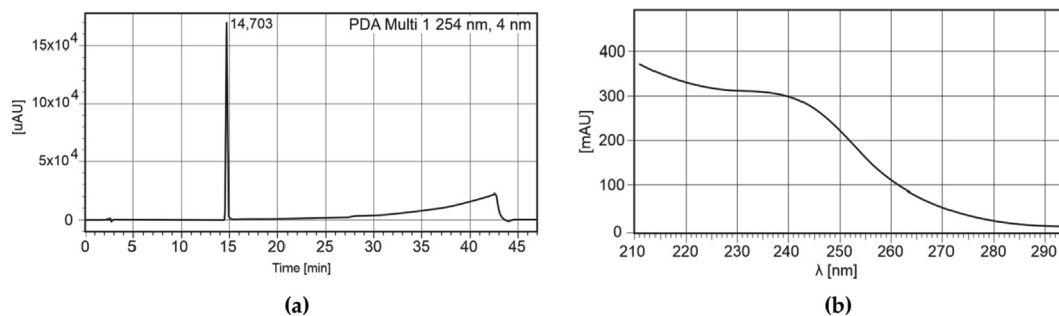


Fig. 8. RDX standard chromatogram (a), UV spectrum of RDX standard at retention time of 14.7 min (b).

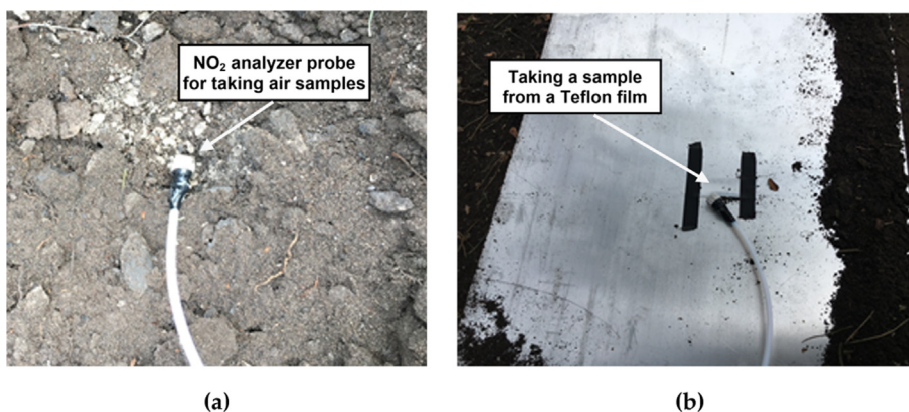


Fig. 9. Photos of air sampling from the ground surface in the crater (a) and from PTFE film attached to metal cover (b).



Therefore, the times from the explosion to the beginning of the first measurement vary from 2 to 16 minutes. The results of the measurements were also significantly influenced by the variable and sometimes strong wind, the speed of which was determined based on data from the local weather station. Measurements of wind speed and directions could be used to determine the place of explosion, which will be subject of further research [26].

### 3.2. Sample No 1: 75 g of TNT

Measurements of  $\text{NO}_2$  concentration, in the distance of 20 m from the explosion site, began 16 minutes after detonation. The wind speed and direction were very variable. All these factors strongly influenced the  $\text{NO}_2$  concentration measurement results (Fig. 10). The graphs show measurements over a 1 minute period to illustrate the effect of wind that is manifested by significant changes in results. Fig. 10a shows the average concentration slightly higher than the  $\text{NO}_2$  concentration normally found in this type of area (approx. 20 ppb). It should be emphasized that more is closer the explosion center, the higher the average  $\text{NO}_2$  concentration. The highest concentrations were recorded in the air sample taken from above PTFE.

### 3.3. Sample No 2: 1 kg of TNT

Measurements related to the sample no 2 started 2 min after detonation. Then the wind speed was lower, and a slightly weaker wind did not significantly affect the results. Therefore, explosive vapors and  $\text{NO}_2$  concentrations were higher in close location to the crater (Fig. 11). As a result, the graphs are flatter and the standard deviation is smaller. In addition, the observation in 1 m from the crater (Fig. 11d) shows significant differences with respect to its center.

### 3.4. Sample No 3: 1 kg of RDX

Measurements presented in Fig. 12a started 3 min after detonation and during this period moderate wind with variable direction

having significantly impact on results causing a  $\text{NO}_2$  concentration increase at a greater distance from the explosion site. This also indicates that the amount of nitrogen dioxide for this type of explosive is in a higher way compared to previous samples, because the increased concentration occurs on a larger area. This test also showed the advantage of using Teflon films. In contrast to previous results, the air taken from PTFE contained the most quantity of  $\text{NO}_2$ , despite the reduced concentration at the explosion center and in the crater. It may be stated that vapor samples adsorbed on this type of film are more stable.

### 3.5. Sample No 4: 0.5 kg of TNT and 0.5 kg of RDX

$\text{NO}_2$  concentrations measurements at the point of 20 m distance started 9 min after detonation. When testing this sample, the wind was strongest and its speed was of 2.8-5.5 m/s. This caused that the cloud of explosive vapors moved from the crater towards the place of measurement in the distance of 20 m and there the concentration of nitrogen dioxide was the highest. In other locations, concentration was almost equal. The high  $\text{NO}_2$  concentration covered a large area, as before, and indicates that the amount of nitrogen dioxide for this type of explosive is high (Fig. 13). These measurements also confirm the usefulness of Teflon films which provide the most stable measurements (the smallest standard deviation).

The results of measurements of  $\text{NO}_2$  concentration for all samples of explosives, taking into account the time between the explosion and measurement as well as the distance from the place of explosion, the temperature and humidity of atmospheric air as well as the wind speed at this time of measurements have been summarized in Table 1.

### 3.6. Soil samples analysis using RP-HPLC

According to the scenario and standard measurement methodology, soil samples were taken from specific points of the explosion crater. Then the analysis was carried out according to the procedures described in Section 2.2. The obtained results of RP-HPLC analysis prove that explosive compounds were present in soil

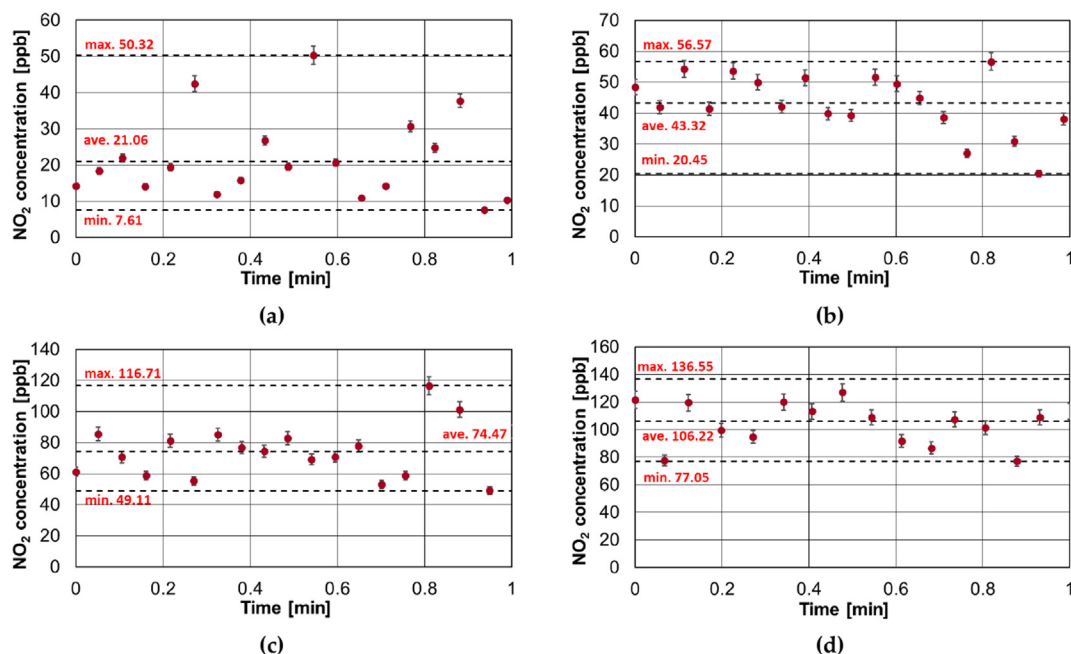
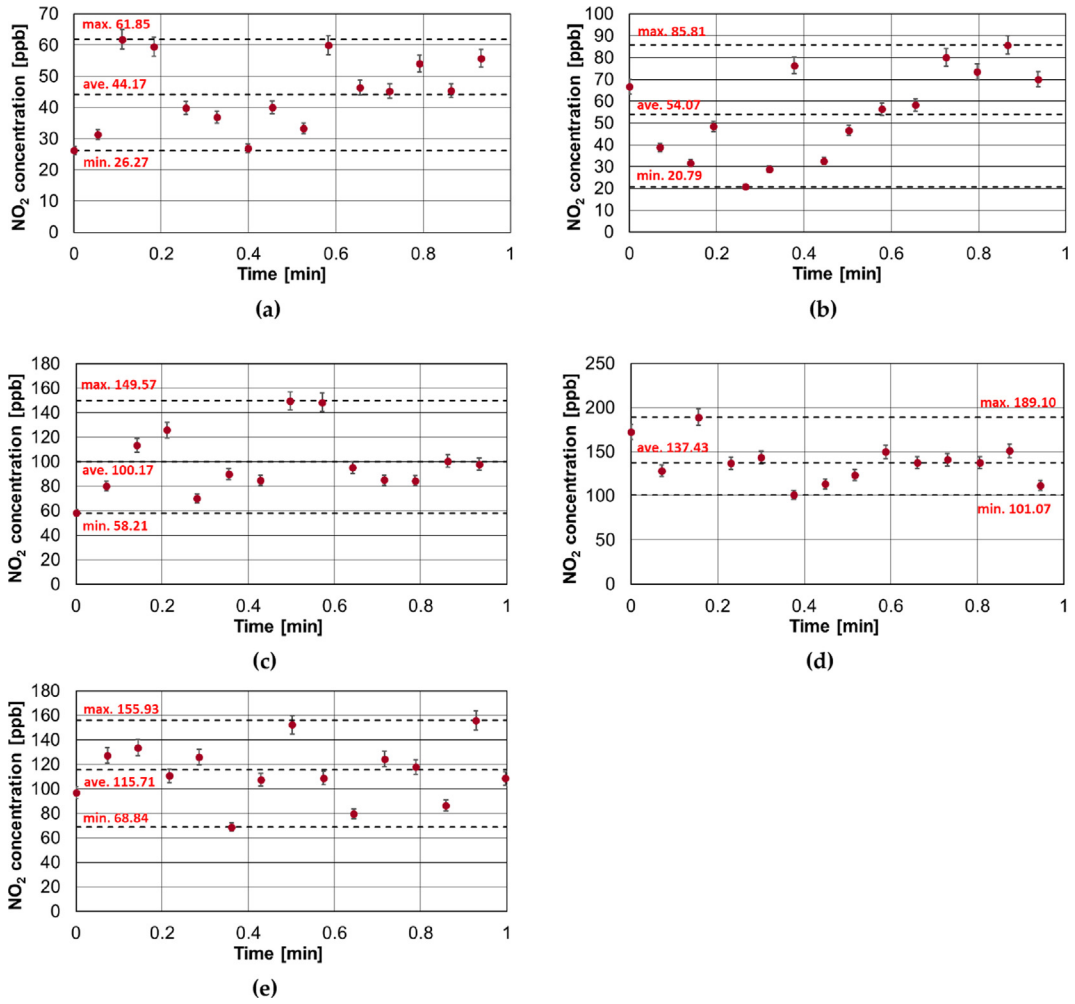
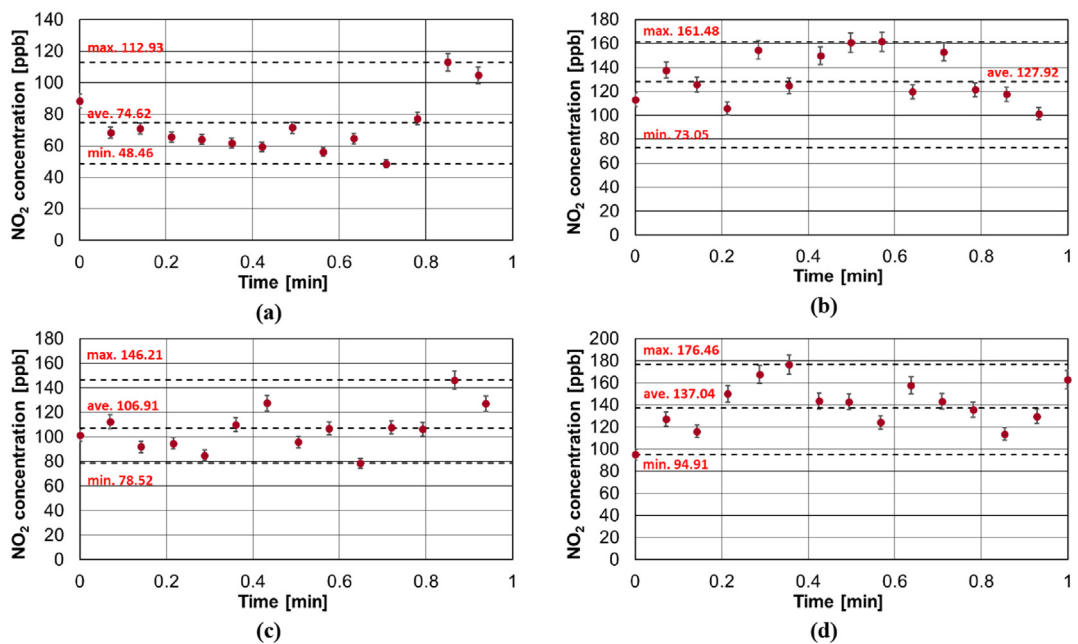


Fig. 10. Results of  $\text{NO}_2$  concentration measurements after an explosion of 75 g of TNT in different distances from the crater: 20 m (a), 10 m (b), 0 m on the ground (c), 0 m on PTFE (d).



**Fig. 11.** Results of NO<sub>2</sub> concentration measurements after an explosion of 1 kg TNT in different distances from the crater: 20 m (a), 10 m (b), 1 m (c), 0 m on the ground (d) and 0 m on PTFE (e).



**Fig. 12.** Results of NO<sub>2</sub> concentration measurements after an explosion of 1 kg of RDX in different distances from the crater: 20 m (a), 10 m (b), 0 m on the ground (c) and 0 m on PTFE (d).

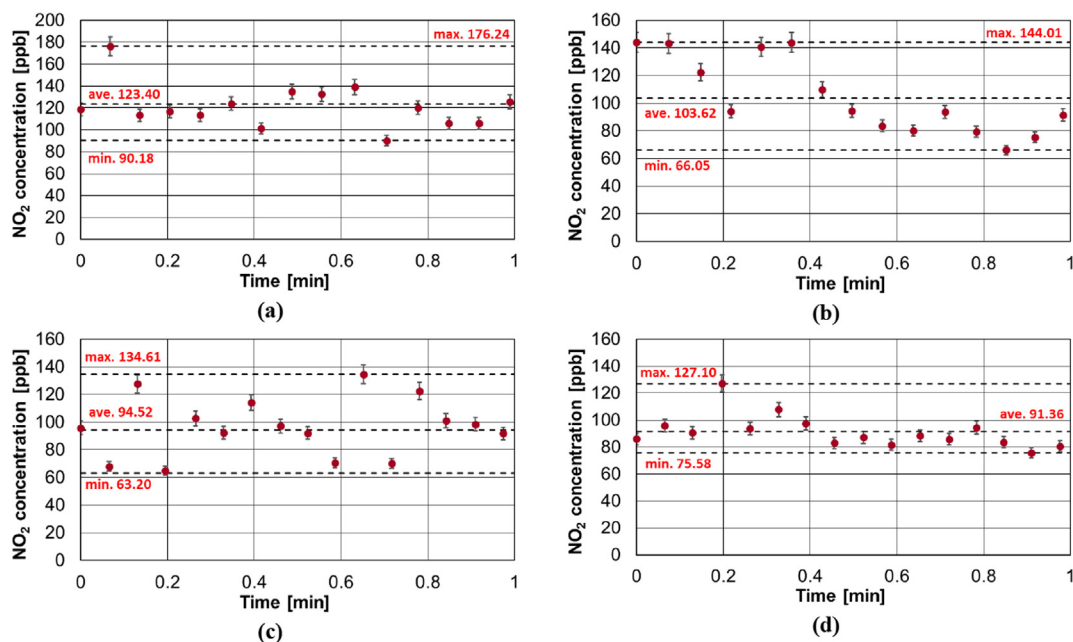


**Fig. 13.** Results of  $\text{NO}_2$  concentration measurements after an explosion of 0.5 kg of TNT and 0.5 kg of RDX in different distances from the crater: 20 m (a), 10 m (b), 0 m on the ground (c) and 0 m on PTFE (d).

**Table 1**

Summary of results, measurement conditions and average  $\text{NO}_2$  concentration in air.

Type of explosives	Time after expl. [min]	Ambient temperature [°]	Humidity RH [%]	Wind [m/s]	Average $\text{NO}_2$ concentration at various locations [ppb]			
					20 m	10 m	0 m	PTFE
75 g TNT	16	10.6	49.1	2.0–5.5	21.06	43.32	74.47	106.22
1 kg TNT	2	11.3	47.8	2.3–5.0	44.17	54.07	137.43	115.71
1 kg RDX	3	11.6	50.3	2.5–5.0	74.62	127.92	106.91	137.04
0.5 kg TNT and 0.5 RDX	9	13.1	47.3	2.8–5.5	123.40	103.62	94.52	91.36

**Table 2**

Results obtained with use of RP-HPLC method.

Type of explosives	Average HEM concentration* at various locations of the crater [ppm]		
	Top	Center	Bottom
75 g TNT	95,5	63,6	34,4
1 kg TNT	27,2	54,8	141,9
1 kg RDX	106,8	83,5	29,9
Mix. 0.5 kg RDX and 0.5 kg TNT	278,9	278,9	434,2
	7117,3	7117,3	124,1

\* Concentration calculated on 100 g of the soil.

samples (see Table 2). Since both TNT and RDX were below the detection limit of the applied apparatus, it was necessary to use the sample concentration procedure that allowed detection of trace residues of explosives in the soil. The soil samples were pre-dissolved in 20 mL of acetone and then centrifuged, filtered through a 0.45  $\mu\text{m}$  PTFE filter, evaporated and dissolved in 0.5 mL of mobile phase – solution of 47.6% acetonitrile (ACN), 47.6%  $\text{H}_2\text{O}$  and 4.8% TFA. As a result, the concentration was 40 times higher and the compounds were correctly identified.

RDX (LOD = 305,1 ppm, LOQ 914 ppm) is less detectable than TNT (LOD = 217 ppm, LOQ = 659 ppm) because of less absorption in UV. An example of a chromatogram of a sample taken after an explosion of sample of 0.5 kg of TNT and 0.5 kg of RDX from the center of an explosive crater (Fig. 14).

#### 4. Discussion

Due to completely different operating principles and measurement procedures, RP-HPLC and CEAS cannot be directly compared. Therefore, for both instruments the signal increase in dB was determined, as the ratio of the maximum signal corresponding to the appearance of the  $\text{NO}_2$  in air (optoelectronic  $\text{NO}_2$  analyzer) or HEM in soil (HPLC) to the background level (Table 3). The HPLC system provides approx. 10 times higher signals, but much more time is needed to get results – even several days, including transport and sample preparation. Results obtained with use of optoelectronic  $\text{NO}_2$  analyzer are in the range of 7.3 dB–8.15 dB, while in HPLC significantly higher result (80.5 dB) was achieved for the fourth sample because the thermodynamics of detonation of the RDX/TNT mixture is worse than in the case of pure TNT or RDX sample. In general, the results obtained in both procedures depend on the physicochemical parameters of the samples (e.g.: HEM composition and stabilizers content, vapor pressure, ED construction), the conditions (e.g.: ground structure) and course of the reaction (initiation and explosion) as well as the measurement conditions. Especially the fact that the moving detonation wave creates low and high pressure zones that affect the spatial distribution of explosive residues and concentration of gaseous detonation products [27].

The optoelectronic  $\text{NO}_2$  analyzer is much faster and allows for initial (screening) hypotheses regarding the source of the explosion



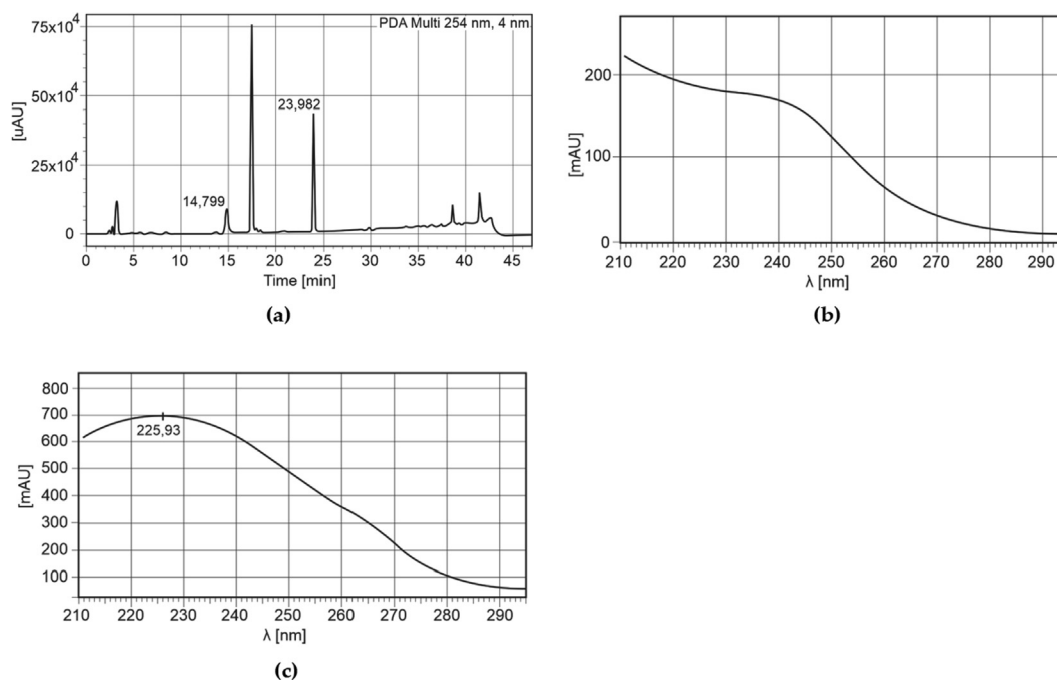


**Fig. 14.** Chromatogram of the concentrated sample of 0.5 kg of TNT and 0.5 kg of RDX taken from the center of the explosion crater (a), UV spectrum of detected compounds at retention time of 14.8 min (b) and 24.0 min (c).

**Table 3**

Table listing comparison of all applied techniques.

Type of explosives	Time analysis using HPLC* [min]	Time analysis using CEAS [min]	HPLC signal increase** [dB]	CEAS signal increase*** [dB]
75 g TNT	50	0.5	60.2	7.3
1 kg TNT			70.2	8.2
1 kg RDX			40.2	8.1
0.5 kg TNT and 0.5 RDX			80.5	7.7

\* Without the time needed to collect and prepare samples.

\*\* Maximum signal increase relative to baseline including 40-fold concentration.

\*\*\* Maximum signal increase relative to baseline.

at the scene of the accident without the need to transport to the lab, used often for tedious procedures for the multi-stage preparation of samples, and long measurement. The use of a pump that would draw in air samples above the tested object at a higher speed, reducing of the analyzer volume and application of concentrator [28], allow for a further analyzer performance improvement. In contrast, HPLC ensures the identification of HEM and other chemical compounds.

## 5. Conclusions

The first demonstration of the  $\text{NO}_2$  analyzer based on cavity enhanced absorption spectroscopy with use of blue-violet laser system to study the explosion site has been presented. Tests related to detect explosives' residues after the detonation of small amounts of nitroaromatic compounds were carried out with use of real charges made from commercially available explosives under field conditions at the training ground. They have shown that these types of analyzers can be complementary to the HPLC soil sample testing equipment, which is a common standard in the analysis of explosives. It should be emphasized that the used RP-HPLC system required to concentrate of the sample 40 times in order to detect and correctly identify the residue of explosives (results after 3 days), while the optoelectronic  $\text{NO}_2$  analyzer provided responses after 30 s, whose amplitudes were about 8 dB despite the fact that  $\text{NO}_2$  in the air was 3 orders of magnitude smaller than explosives

found in soil. Therefore such analyzers can be a useful tool providing fast results and search for the scene of the incident, even in a windy day, and without the need for special sampling and delivery to the analytical laboratory. To further improve the detection ability of the analyzer, the so-called concentrator providing adsorption and decomposition of explosives vapor can be considered. In the next step of identification of the explosives detection capabilities by means of laser absorption spectroscopy other type of explosives including liquids ones will be studied.

## Funding

The field tests was funded by the Science for Peace Programme of NATO, Grant no. G5147. Research carried out in the laboratory of Institute of Optoelectronics MUT was financially supported by the Polish MoD within research grant no. GBMON/13-993/2018/WAT.

## CRediT authorship contribution statement

**Jacek Wojtas:** Conceptualization, Methodology, Validation, Formal analysis, Investigation, Resources, Writing - original draft, Writing - review & editing, Visualization, Funding acquisition. **Robert Bogdanowicz:** Conceptualization, Investigation, Writing - review & editing, Funding acquisition. **Agata Kamienska Duda:** Resources, Investigation, Formal analysis, Validation, Writing - review & editing. **Beata Pietrzyk:** Writing - review & editing.

**Michał Sobaszek:** Resources, Investigation. **Piotr Prasała:** Resources, Investigation, Formal analysis. **Anna Dettlaff:** Resources, Investigation. **Krzysztof Achtenberg:** Software, Resources, Investigation.

### Declaration of Competing Interest

The authors declare that they have no known competing financial interests or personal relationships that could have appeared to influence the work reported in this paper.

### References

- [1] A. Beveridge, Forensic Investigation of Explosions, CRC Press, 2011, <https://doi.org/10.1201/b11938>.
- [2] K.W. Busch, M.A. Busch (Eds.), Cavity-Ringdown Spectroscopy, American Chemical Society, Washington, DC, 1999, <https://doi.org/10.1021/bk-1999-0720>.
- [3] J. Wojtas, T. Stacewicz, Z. Bielecki, B. Rutecka, R. Medrzycki, J. Mikołajczyk, Towards optoelectronic detection of explosives, Opto-Electronics Rev. 21 (2013) 210–219, <https://doi.org/10.2478/s11772-013-0082-x>.
- [4] United States Environmental Protection Agency, Method 8330A: Nitroaromatics and nitramines by high performance liquid chromatography (HPLC); Revision 1, Washington DC. <https://www.epa.gov/sites/production/files/2015-12/documents/8330a.pdf>, 2007 (accessed on January 2020).
- [5] EPA-RCA, Method 8330B: Nitroaromatics, nitramines, and nitrate esters by high performance liquid chromatography (HPLC); Revision 2, Washington DC. <https://www.epa.gov/sites/production/files/2015-07/documents/epa-8330b.pdf>, 2006 (accessed on January 2020).
- [6] D. Gaurav, A.K. Malik, P.K. Rai, High-Performance Liquid Chromatographic Methods for the Analysis of Explosives, Crit. Rev. Anal. Chem. 37 (2007) 227–268, <https://doi.org/10.1080/10408340701244698>.
- [7] U. Nyberg, V. Klippmark, H. Karlström, A. Beyglou, N. Petropoulos, Short time measurements of toxic fumes from detonation of emulsion explosive, Swedrec Report 2015 (2015) 1.
- [8] R.J. Mainiero, J.H. Rowland III, M.L. Harris, M.J. Sapko, Behavior of Nitrogen Oxides in the Product Gases from Explosive Detonations, Proc. 32nd Annu. Conf. Explos. Blasting Tech., Texas USA, 2006.
- [9] M. Sapko, J. Rowland, R. Mainiero, I. Zlochower, Chemical and physical factors that influence NO<sub>x</sub> production during blasting - Exploratory study, in: Proc. Annu. Conf. Explos. Blasting Tech., 2002, pp. 317–330.
- [10] I. Zawadzka-Małota, Testing of mining explosives with regard to the content of carbon oxides and nitrogen oxides in their detonation products, J. Sustain. Min. 14 (2015) 173–178, <https://doi.org/10.1016/j.jsm.2015.12.003>.
- [11] P. Dowker, P. Walsh, Real-time measurement of nitrogen monoxide in tunnels and its oxidation rate in diluted diesel exhaust, Executive Health and Safety, 2009.
- [12] M.C. Phillips, B.E. Brumfield, B.E. Bernacki, S.S. Harilal, J.M. Schwallier, N.G. Glumac, Broadband Infrared Laser Absorption Spectroscopy of High-Explosive Detonations, in: 2019 Conf. Lasers Electro-Optics, CLEO 2019 - Proc., 2019, pp. 4–5. <https://doi.org/10.23919/CLEO.2019.8750529>.
- [13] M.C. Phillips, B.E. Bernacki, S.S. Harilal, B.E. Brumfield, J.M. Schwallier, N.G. Glumac, Characterization of high-explosive detonations using broadband infrared external cavity quantum cascade laser absorption spectroscopy, J. Appl. Phys. 126 (2019), <https://doi.org/10.1063/1.5107508>.
- [14] Y. Yamamoto, H. Sumizawa, H. Yamada, K. Tonokura, Real-time measurement of nitrogen dioxide in vehicle exhaust gas by mid-infrared cavity ring-down spectroscopy, Appl. Phys. B. 105 (2011) 923–931, <https://doi.org/10.1007/s00340-011-4647-4>.
- [15] K. Liu, R. Lewicki, F.K. Tittel, Development of a mid-infrared nitrogen dioxide sensor based on Faraday rotation spectroscopy, Sens. Actuat. B Chem. 237 (2016) 887–893, <https://doi.org/10.1016/j.snb.2016.07.020>.
- [16] R. Sur, W.Y. Peng, C. Strand, R. Mitchell Spearrin, J.B. Jeffries, R.K. Hanson, A. Bekal, P. Halder, S.P. Poonacha, S. Vartak, A.K. Sridharan, Mid-infrared laser absorption spectroscopy of NO<sub>2</sub> at elevated temperatures, J. Quant. Spectrosc. Radiat. Transf. 187 (2017) 364–374, <https://doi.org/10.1016/j.jqsrt.2016.10.016>.
- [17] S. Voigt, J. Orphal, J.P. Burrows, The temperature and pressure dependence of the absorption cross-sections of NO<sub>2</sub> in the 250–800 nm region measured by Fourier-transform spectroscopy, J. Photochem. Photobiol. A Chem. 149 (2002) 1–7, [https://doi.org/10.1016/S1010-6030\(01\)00650-5](https://doi.org/10.1016/S1010-6030(01)00650-5).
- [18] A. Karpf, G.N. Rao, High sensitivity detection of NO<sub>2</sub> using ICOS and MLIAS, in: CLEO2011 - Laser Appl. to Photonic Appl., OSA, Washington, D.C., 2011, pp. JTul113. [https://doi.org/10.1364/CLEO\\_AT.2011.JTu1113](https://doi.org/10.1364/CLEO_AT.2011.JTu1113).
- [19] J. Wojtas, Z. Bielecki, Signal processing system in cavity enhanced spectroscopy, Opto-Electronics Rev. 16 (2008), <https://doi.org/10.2478/s11772-008-0034-z>.
- [20] R. Engeln, G. Berden, R. Peeters, G. Meijer, Cavity enhanced absorption and cavity enhanced magnetic rotation spectroscopy, Rev. Sci. Instrum. 69 (1998) 3763–3769, <https://doi.org/10.1063/1.1149176>.
- [21] H. Akimoto, Atmospheric Reaction Chemistry, Springer Japan (2016), <https://doi.org/10.1007/978-4-431-55870-5>.
- [22] Y.M. Taha, C.A. Odame-Ankrah, H.D. Osthoff, Real-time vapor detection of nitroaromatic explosives by catalytic thermal dissociation blue diode laser cavity ring-down spectroscopy, Chem. Phys. Lett. 582 (2013) 15–20, <https://doi.org/10.1016/j.cplett.2013.07.040>.
- [23] Y.M. Taha, M.T. Saowapon, H.D. Osthoff, Detection of triacetone triperoxide by thermal decomposition peroxy radical chemical amplification coupled to cavity ring-down spectroscopy, Anal. Bioanal. Chem. 410 (2018) 4203–4212, <https://doi.org/10.1007/s00216-018-1072-0>.
- [24] J. McKinley, R.E. Majors, The Preparation of Calibration Standards for Volatile Organic Compounds— A Question of Traceability, La Marque, TX 77568 USA, 2000. <https://kin-tek.com/articles/> (accessed on January 2020).
- [25] ASTM D5143-06(2015)e1, Standard Test Method for Analysis of Nitroaromatic and Nitramine Explosive in Soil by High Performance Liquid Chromatography, 2015, ASTM International. <https://www.astm.org> (accessed on January 2020).
- [26] E.J. Zhang, C.C. Teng, T.G. van Kessel, L. Klein, R. Muralidhar, G. Wysocki, W.M.J. Green, Field Deployment of a Portable Optical Spectrometer for Methane Fugitive Emissions Monitoring on Oil and Gas Well Pads, Sensors. 19 (2019) 2707, <https://doi.org/10.3390/s19122707>.
- [27] J.P. Agrawal, High Energy Materials: Propellants, Explosives and Pyrotechnics, Wiley-VCH, Weinheim, Germany, 2010.
- [28] J. Wojtas, B. Rutecka, S. Popiel, J. Nawala, M. Wesołowski, J. Mikołajczyk, S. Cudziło, Z. Bielecki, Explosives Vapors-Concentrating and Optoelectronic Detection, Metrol. Meas. Syst. 21 (2014) 177–190, <https://doi.org/10.2478/mms-2014-0016>.

